Nonequilibrium Phase Transitions of Vortex Matter in Three-Dimensional Layered Superconductors

Qing-Hu Chen^{1,2} and Xiao Hu¹

¹ Computational Materials Science Center, National Institute for Materials Science, Tsukuba 305-0047, Japan
² Department of Physics, Zhejiang University, Hangzhou 310027, P. R.China
(October 26, 2018)

Large-scale simulations on three-dimensional (3D) frustrated anisotropic XY model have been performed to study the nonequilibrium phase transitions of vortex matter in weak random pinning potential in layered superconductors. The first-order phase transition from the moving Bragg glass to the moving smectic is clarified, based on thermodynamic quantities. A washboard noise is observed in the moving Bragg glass in 3D simulations for the first time. It is found that the activation of the vortex loops play the dominant role in the dynamical melting at high drive.

74.60.Ge, 74.50.+r, 74.40.+k

Dynamical properties of current driven vortex matter^{1,2,3} interacting with random pinning potentials in type II superconductors have attracted considerable attention both experimentally^{4,5,6,7,8} and theoretically. 9,10,11,12 A better understanding of various nonequilbrium phases and phase transitions is essential for explaining the nonlinear current-voltage (I-V) characteristics observed in experiments conducting on samples in an external magnetic field, 4,13 which is known as the first evidence of the first-order vortex lattice melting. In addition, this problem is closely related to an important class of phenomena in condensed matter physics, such as dynamics of sliding charge-density waves (CDW) in quasi-one-dimensional conductors, ¹⁴ Wigner crystals in a two-dimensional (2D) electron gas, ¹⁵ as well as driven interface in random media.¹⁶

Vortex matter shows the three regimes of creep, depinning, and flow in its transport characteristics, depending on the drive. In the flow regime, the periodicity in the direction transverse to motion leads to a novel phase: moving Bragg glass (BrG), based on an elastic transverse equation of motion proposed by Giamarchi and Le Doussal (GL). As the driven force is reduced, the effective pinning strength becomes larger. It has been argued that moving vortex matter may decay first into a moving smectic 10,11 and then into a moving liquid. It can be further driven into a creeping BrG below the depinning threshold. Recently, these moving phases have been observed both experimentally 5,6 and in numerical simulations. 19,20,21,22,23,24,25

A precise analytical description is very challenging, especially in the transition regime, because it is quite difficult to deal with the topological defects¹⁸ in the plastic flow. Even within the elastic approach, an analytical study of driven vortex matter is hampered by dynamic nonlinearities such as Kardar-Parisi-Zhang term¹⁷ that governs the vortex dynamics on large scale. The underlying mechanism of the dynamical melting still remains open question. In recent years, several three-dimensional (3D) numerical simulations have been performed.^{23,24,25}

However, one common shortage is that the moving BrG holds out to arbitrary high drives, which is obviously contradictory to any real experiments.

In the present Letter, we report new results of nonequilibrium simulations for vortex matter in anisotropic 3D systems with weak disorder. The dynamical melting from the moving BrG to the moving smectic is found to be first order. The washboard noise is observed in the voltage power spectra in the moving BrG. Our results suggest that the thermally activated vortices play a dominant role in the dynamical melting at high currents.

Vortex matter in type II layered superconductors can be described by the 3D anisotropic XY model on a simple cubic lattice 26,27,28

$$H = -\sum_{\langle ij\rangle} J_{ij} \cos(\phi_i - \phi_j - A_{ij}), \tag{1}$$

where ϕ_i specifies the phase of the superconducting order parameter on site $i, \ A_{ij} = (2\pi/\Phi_0) \int_i^j {\bf A} \cdot {\bf dl}$ with ${\bf A}$ the magnetic vector potential of a field $\mathbf{B} = \nabla \times \mathbf{A}$ along the z axis. The random pinning potential is introduced in the coupling strength in the xy plane $J_{ij} = J_0(1 + p\epsilon_{ij})$, where ϵ_{ij} 's are independently Gaussian distributed with zero mean and unit variance, p represents the pinning strength.²⁸ The coupling between the xy planes is $J_z =$ J_0/Γ^2 , (Γ is the anisotropy constant). This model is relevant to high- T_c superconductors and artificially layered superconductors. For the data presented below, we typically choose p = 0.04 which models weak pinning strength, $1/\Gamma^2 = 1/40$, and the average number of vortex lines per plaquette $f = l^2 B/\Phi_0 = 1/20$, where l is grid spacing in the ab plane. Our system size is L=40for all directions.

In order to study the transport properties, we incorporate the Resistivity-Shunted-Junction dynamics in simulations. Realizing that the sum of supercurrents into site i can be expressed in terms of the derivative of Eq. (1) with respect to ϕ_i , the dynamical equations for the ϕ 's are readily derived by requiring the sum of currents into each site to vanish

$$\frac{\sigma\hbar}{2e} \sum_{i} (\dot{\phi}_i - \dot{\phi}_j) = -\frac{\partial H}{\partial \phi_i} + J_{\text{ext},i} - \sum_{i} \eta_{ij}, \qquad (2)$$

where $J_{\text{ext},i}$ is the external current which vanishes except for the boundary sites. The η_{ij} is the thermal noise current with zero mean and a correlator $\langle \eta_{ij}(t)\eta_{ij}(t')\rangle = 2\sigma k_B T \delta(t-t')$. In the following, the units are taken of $2e = J_0 = \hbar = \sigma = 1$.

In the present simulation, a uniform external current I_x along x -direction is fed into the system. The fluctuating twist boundary condition²⁹ is applied in the xy plane to maintain the current, and the periodic boundary condition is employed in the z axis. In the xy plane, the supercurrent between sites i and j is now given by $J_{i\rightarrow j}^{(s)}=J_{ij}\sin(\theta_i-\theta_j-A_{ij}-\mathbf{r}_{ij}\cdot\boldsymbol{\Delta}),$ with $\boldsymbol{\Delta}=(\Delta_x,\Delta_y)$ the fluctuating twist variable and $\theta_i=\phi_i+\mathbf{r}_i\cdot\boldsymbol{\Delta}.$ The new phase angle θ_i is periodic in both x- and y-directions. Dynamics of $\boldsymbol{\Delta}$ can be then written as

$$\dot{\Delta}_{\alpha} = \frac{1}{L^3} \sum_{\langle ij \rangle_{\alpha}} \left[J_{i \to j}^{(s)} + \eta_{ij} \right] - I_{\alpha},\tag{3}$$

where $\alpha = x, y$. The voltage drop is $V = -L\dot{\Delta}_x$.

The above equations can be solved efficiently by a pseudo-spectral algorithm³⁰ due to the periodicity of phase in all directions. The time stepping is done using a second-order Runge-Kutta scheme with $\Delta t = 0.05$. Our runs are typically $(4 \sim 8) \times 10^7$ time steps and the latter half time steps are for the measurements. For a given current, the simulations are started from high temperatures with random initial phase configurations, and vortex systems are gradually cooled down. The present results are based on one realization of disorder. For these parameters, the equilibrium BrG melts to a liquid at $T = 0.254^{28}$ and the critical current $I_c(T = 0)$ is estimated to be around 0.095. We calculate the internal energy e per flux line per layer, the helicity modulus alongthe z axis Υ_z , and the vortex structure factor in the xy plane, together with the density of dislocations ρ_d and vortex-antivortex pairs ρ_{av} in the xy plane. The helicity modulus describes the superconducting phase coherence.

As shown in Fig. 1, evident jump of e is observed around the melting temperature T_m for I=0.5, which clearly indicates a first-order dynamical melting. The helicity modulus Υ_c is very sharply set up precisely at T_m , consistent with the first-order nature. The vanish of Υ_z above T_m shows that the dynamical melting marks the loss of superconducting phase coherence along the z direction.

To characterize the spatial order of moving phases, we show the structure factors in the vicinity of T_m at various currents in Fig. 2. At high currents I = 0.5 and $0.3 \gg I_c(0)$, moving BrG's with six well-defined peaks are found just below T_m , which shows the quasi-long-range translational correlations both perpendicular and parallel to the flow direction, consistent with the predictions by GL.¹⁰ By mapping out the trajectories of the

moving vortices, we found a set of periodic coupled elastic channels, corresponding to peaks in the $K_y=0$ axis. The peak in $K_y\neq 0$ is anisotropic. The half width along the flow direction is considerably smaller than that transverse to the flow, indicating that the positional correlation along the flow direction is much stronger than that transverse to the flow, which provides a solid base for the moving BrG theory, 10 where a long range order is assumed along the flow direction.

One can see from Figs. 2 (a) and (b) that the moving BrG melts sharply into a moving smectic just above T_m where Bragg peaks only remain in $K_y = 0$ axis, confirming the proposal by Balents et al.¹¹ The current dependent anisotropy of the smectic peak will be discussed later. The moving smectic was unnoticed in a previous simulation²² using isotropic 3D XY model for higher vortex density with smaller system size. In addition, the orientation of vortex lattice was found to be not aligned with the direction of the motion,²² inconsistent with the characterization of the moving BrG.

Through extensive simulations in vortex flow regime, we universally find that the appearance of a moving smectic is simultaneously accompanied by the loss of the superconducting phase coherence along the z direction ($\Upsilon_z = 0$). It demonstrates that the vortices flow incoherently in different xy planes in a moving smectic.

As the temperature further increases, the moving smectic continuously evolves into a moving liquid with a ringlike pattern in the structure factor (not shown here). We have not found any anomaly in e, demonstrating a continuous phase transition. In low current regime, e.g. $I=0.05~(\ll I_c(0))$, it is found in Fig. 2(c) that the (creeping) BrG directly melts to a liquid without through an intermediate moving smectic, close to equilibrium.

To capture insight of the underlying mechanism of the dynamical melting, we display temperature dependence of the density of dislocations ρ_d in Fig. 3. Sharp jump of ρ_d right at T_m demonstrates that the dynamical melting is mediated by the proliferation of dislocations, analogous to the equilibrium melting²⁷. Dislocations can be created either by entanglement of the field-induced flux lines or by excitations of small vortex loops, the latter could be more important in the presence of external currents. For I = 0.3, we find that vortex loops are only activated far above T_m , which excludes the effect of vortex loops in the melting. Anisotropy of the smectic peak at this current exhibited in Fig. 2(b) is therefore quite similar to that in Ref. (19) without the mechanism to generate vortex loops. However, at I = 0.5, the thermally activated vortices play an essential role in the dynamical melting. The density of thermally excited vortices ρ_{av} also shows a steep jump at T_m . The smearing out of the smectic peak transverse to the flow at I = 0.5 shown in Fig. 2(a) is just originated from the nucleation of vortex loops. As the current increases to 0.69, "thermally" activated vortex-antivortex pairs remain down to zero temperature. Above this current, the superconducting coherence along the z direction vanish at any temperature. In this sense, we refer this current to a depairing critical current. It is just the thermally activated vortex loops that induce dislocations, which in turn destroy the superconducting moving BrG in very high currents. The perturbation of these excited vortex loops has not been considered in the analytical theories. ^{10,11,12} In previous simulations using Langvein dynamics of a fixed number of interacting particles, ^{19,20,21,23,24,25} the effect of thermally activated vortices are absolutely excluded, so the moving BrG remains unreasonably in arbitrary high currents.

Repeating such simulations at various currents, we compose a dynamical phase diagram of vortex matter as a function of I and T in Fig. 4. The continuous phase transition from the moving smectic to the moving liquid is determined by criterion that the smectic peak height from the ring background is less than 0.05. $T_m(I)$ is always lower than $T_m(0)$ and shows a nonmonotonic characteristics. This naturally bring about the possibility of the reordering of driven vortex matter with the increase of drives predicted theoretically.

To show the temporal correlation in BrG phase, we calculate the power spectra of voltage noise $s(\omega) =$ $\left|\int V_x(t)e^{-i2\pi\omega t}dt\right|^2$. In Fig. 5(a), well-developed peaks appear at the washboard frequency and harmonics for I=0.3 at T=0. The voltage noise spectrum for I=0.5at T=0 is also presented in the inset of Fig. 5(a) for comparison. The voltage cross the sample is $V_x(t) \propto nv_y$, where n is the vortex density and v_y is the vortex velocity in the y direction.³¹ The washboard frequency is given by $\omega_0 = v_y/a$, where a is the vortex spacing. Due to the same vortex density, we really find that the voltage ratio (≈ 2.01) is exactly consistent with that of two washboard frequencies. As the temperature increases, as shown in Fig. 5(b), the peak at ω_0 remains in all moving BrG phases and suddenly disappears just above T_m . The moving BrG phase is then characterized by the peak at ω_0 . Interestingly, we find that the peak at $\omega = 5\omega_0$ owing to the network discretization is gone in temperatures far below T_m , which excludes the effect of the artificial lattice pinning in the phase transition. In the moving smectic, the short range of the position correlation along the flow direction totally destroys the temporal order of the moving vortices. To the best of our knowledge, the washboard noise, observed recently in both conventional⁷ and high- T_c superconductors, 8 has never been reported in numerical simulations except in 2D at zero temperature.²¹ We believe this to be the first observation of the washboard velocity modulation of driven vortex matter in 3D numerical simulations.

We acknowledge useful discussions with A. Maeda, Y. Nonomura, L. H. Tang, A. Tanaka, and H. H. Wen. The present simulations were performed on the Numerical Materials Simulator (SX-5) in NIMS, Japan. This study was supported by the Ministry of Education, Culture, Sports, Science and Technology, Japan, under the Priority Grant No. 14038240. One of us (QHC) was partially

supported by the JSPS invitation program and the NSFC under Grant No. 10075039 & 10274067.

- ¹ G. Blatter et al., Rev. Mod. Phys. **66**, 1125(1994).
- ² T. Nattermann and S. Scheidl, Adv. Phys. **49**, 607(2000).
- ³ For a recent review, see T. Giamarchi and S. Bhattacharya, cond-mat/0111052.
- ⁴ S. Bhattacharya and M. J. Higgins *et al.*, Phys. Rev. Lett. **70**, 2617(1993).
- ⁵ M. Marchevsky *et al.*, Phys. Rev. Lett. **78**, 531 (1997).
- ⁶ F. Pardo *et al.*, Nature (London) **396**, 348 (1998).
- ⁷ A. M. Troyanovski *et al.*, Nature (London) **399**, 665 (1999).
- ⁸ Y. Togawa *et al.*, Phys. Rev. Lett. **85**, 3716 (2000); A. Maeda *et al.*, Phys. Rev. B **65**, 054506(2001).
- ⁹ A. E. Koshelev and V. M. Vinokur, Phys. Rev. Lett. **73**, 3580 (1994).
- T. Giamarchi and P. Le Doussal, Phys. Rev. Lett. **76**, 3408 (1996); ibid. **78**, 752 (1997); P. Le Doussal and T. Giamarchi, Phys. Rev. B **57**, 11 356 (1998).
- ¹¹ L. Balents *et al.*, Phys. Rev. Lett. **78**, 751 (1997); Phys. Rev. B **57**, 7705 (1998).
- ¹² S. Scheidl and V. M. Vinokur, Phys. Rev. B **57**, 13 800 (1998).
- H. Safar et al., Phys. Rev. B 52, 6211(1995); M. C. Hellerqvist et al., Phys. Rev. Lett. 76, 4022 (1996); J. A. Fendrich et al., ibid. 77, 2703 (1996); D. T. Fuchs et al., ibid. 81, 3944 (1998).
- ¹⁴ G. Grüner, Rev. Mod. Phys. **60**, 1129(1988).
- ¹⁵ E. Y. Andrei *et al.*, Phys. Rev. Lett. **60**, 2765(1988).
- ¹⁶ O. Narayan and D.S. Fisher, Phys. Rev. Lett. **68**, 3515 (1992); T. Nattermann *et al.*, J. Phys. II **2**, 1483 (1992).
- ¹⁷ M. Kardar *et al.*, Phys. Rev. Lett. **56**, 889 (1986).
- ¹⁸ S. Scheidl and V. M. Vinokur, Phys. Rev. **56**, R8522(1997);
 J. Kierfeld *et al.*, Phys. Rev. Lett. **85**, 4948 (2000).
- ¹⁹ K. Moon et al., Phys. Rev. Lett. **77**, 2778(1996).
- ²⁰ S. Ryu *et al.*, Phys. Rev. Lett. **77**, 5114(1996); H. Fangohr *et al.*, Phys. Rev. B **64**, 064505(2001).
- ²¹ C. J. Olson *et al.*, Phys. Rev. Lett. **81**, 3757 (1998); A. B. Kolton *et al.*, ibid. **83**, 3061 (1999);ibid. **86**, 4112 (2001).
- ²² D. Domínguez et al., Phys. Rev. Lett. 78, 2644 (1997).
- ²³ A. van Otterlo*et al.*, Phys. Rev. Lett. **84**, 2493 (2000).
- ²⁴ C. J. Olson *et al.*, Phys. Rev. Lett. **85**, 5416(2000); Phys. Rev. B **64**, 140502 (2001).
- ²⁵ A. B. Kolton *et al.*, Phys. Rev. B **62**, R14657(2000).
- ²⁶ X. Hu *et al.*, Physica (Amsterdam) **282-287C**, 2057(1997);
 Phys. Rev. Lett. **79** , 3498(1997); Phys. Rev. B **58**, 3438(1998).
- ²⁷ Y. Nonomura and X. Hu, Phys. Rev. Lett. **86**, 5140 (2001).
- ²⁸ P. Olsson and S. Teitel, Phys. Rev. Lett. **87**, 137001(2001).
- ²⁹ B. J. Kim, P. Minnhagen and P. Olsson, Phys. Rev. B **59**, 11506(1999).
- ³⁰ Q. H. Chen, L. H. Tang, and P. Q. Tong, Phys. Rev. Lett. 87, 067001(2001); L. H. Tang and Q. H. Chen, Physica B 279, 227(2000).
- 31 J. Bardeen and M. J. Stephen, Phys. Rev. 140, A1197

(1965).

Fig. 1. Temperature dependence of internal energy e (cycles) and helicity modulus along the z axis Υ_z (squares) at I=0.5.

Fig. 2. The vortex structure factors just above and below T_m for (a) T = 0.5, (b) T = 0.3, and (c) T = 0.05.

Fig. 3. Temperature dependence of the density of dislocations ρ_d and thermally activated vortex-antivortex pairs ρ_{av} at various currents.

Fig. 4. Dynamical phase diagram in temperaturecurrent plane. Solid lines with open cycles: 1^{st} order (dynamical) melting from moving BrG to smectic. Dashed lines: continuous phase transition from the moving smectic to liquid.

Fig. 5. Voltage noise power spectra $s(\omega)$ for I=0.3 at (a) T=0, (b) T=0.118, and for I=0.5 at T=0 in the inset of (a).

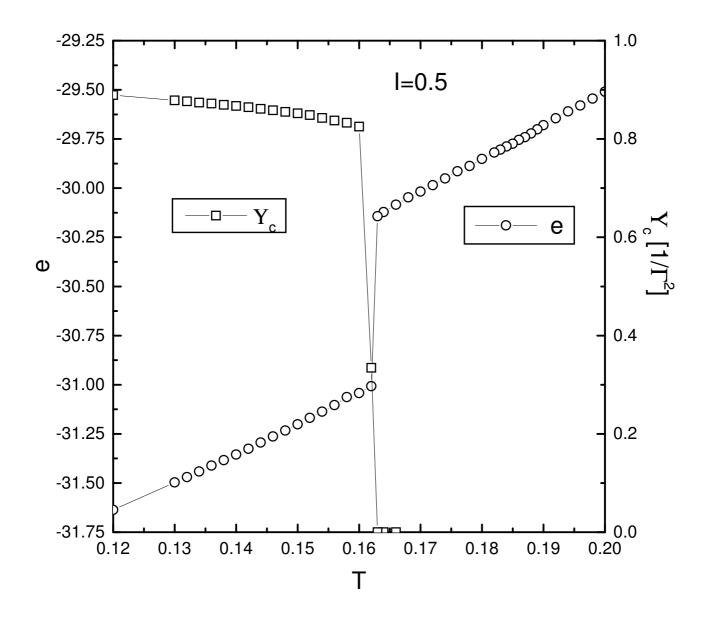
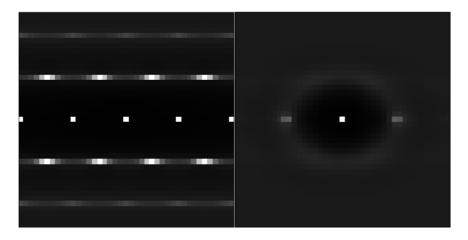
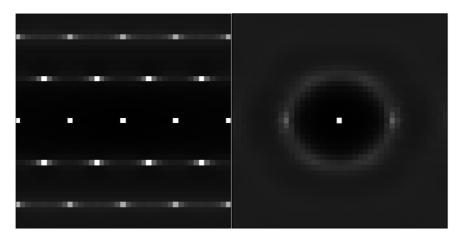


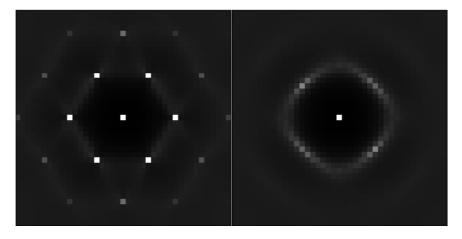
Fig. 1 Chen et al.



(a) I=0.5, T=0.162(left) and T=0.164 (right)



(b) I=0.3 , T=0.118(left) and T=0.120 (right)



(c) I=0.05 , T=0.236(left) and T=0.238 (right) $\label{eq:Fig.2.Chen} \text{Fig.2.Chen et al.}$

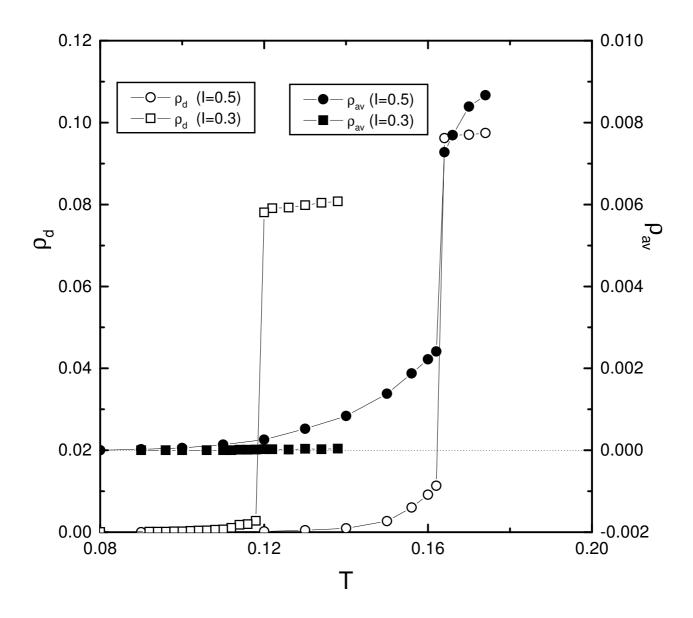


Fig. 3. Chen et al.

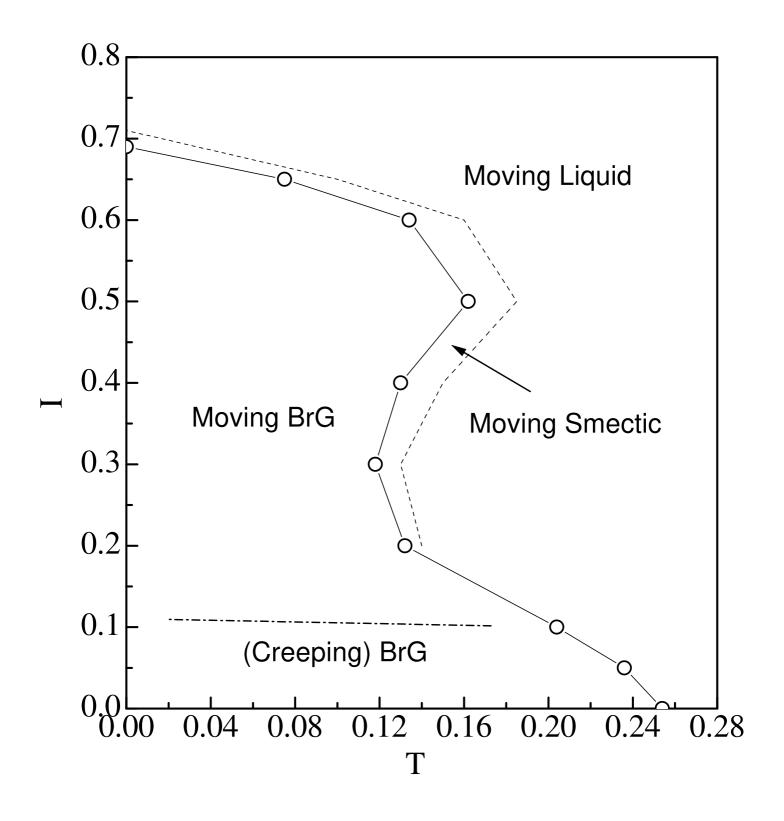


Fig. 4 Chen et al.

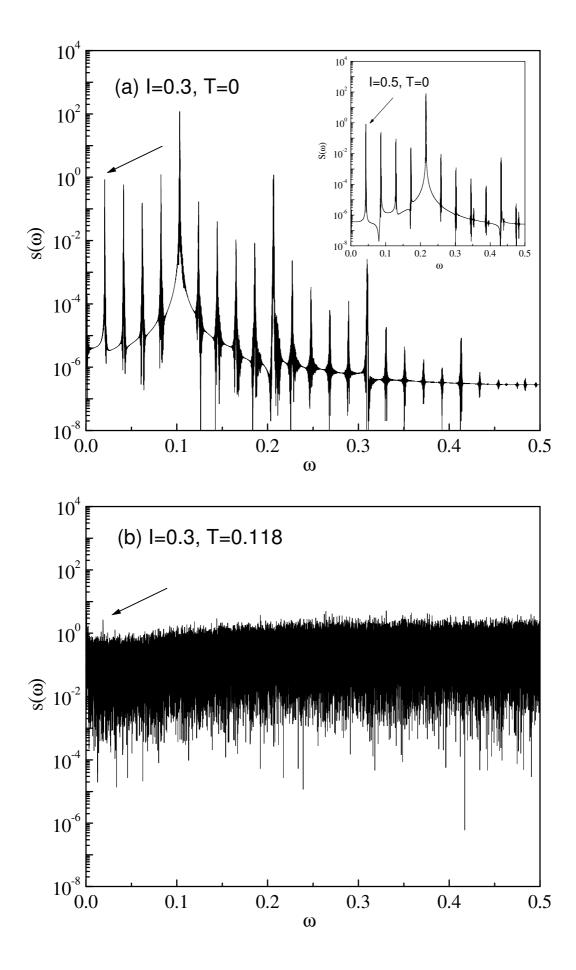


Fig.5. Chen et al.